Binder free boron nitride-based coatings deposited on mild steel by chemical vapour deposition: Anti-corrosion performance analysis

Aamir Nadeem [a], Muhammad Faheem Maqsood [a], Mohsin Ali Raza [a,*], Muhammad Tasaduq Ilyas [a], Muhammad Javaid Iqbal [b], Zaeem Ur Rehman [a]

[a] Deparment of Metallurgy and Materials Engineering, Faculty of Engineering and Technology, University of the Punjab, Lahore, Pakistan
[b] Centre of Excellence for Solid State Physics, University of the Punjab, Lahore, Pakistan

ARTICLE INFO

ABSTRACT

Boron nitride-based coating was deposited on mild steel (MS) substrate by the chemical reaction of boron powder and ammonia gas in a chemical vapour deposition setup at 1200 °C. The effect of reaction temperature and time were studied to obtain uniform coating on MS. A uniform BN-coating was obtained for the reaction time of 1 and 3 h at 1200 °C. The as-deposited boron nitride (BN) coating was characterized by Fourier transform infrared spectroscopy, X-ray diffraction (XRD), scanning electron microscopy (SEM) and atomic force microscopy (AFM). The anti-corrosion performance of the coating was studied by Tafel analysis and electrochemical impedance spectroscopy (EIS) in 3.5% NaCl solution. XRD analysis confirmed that the coating consisted of hexagonal BN. SEM analysis revealed presence of mainly boron nitride nanosheets (BNNS). However, some tubular and ribbon like structures along with some pores were also observed in the as-deposited coating. AFM analysis confirmed that coating consisted of BNNS with thickness of 5–6 nm. EIS analysis showed charge transfer resistance of bare MS and BNNS coated-MS were 298.8 and 1996.3 Ωcm^2, respectively, suggesting BNNS coating had $6 \times$ times higher resistance to saline corrosion than bare MS.

1. Introduction

Adequate metallic corrosion prevention measures are keys for preservation of infrastructure and economy. Surface protection of metals by coatings is an important and widespread corrosion prevention technique which worth billions of dollars market [1]. Coatings, commonly based on metals, ceramics and polymers [2,3] are selected on the basis of nature of substrate, service environment, longevity and cost. Thanks to rapid advancement of nanotechnology, new coatings have emerged for corrosion protection of metals. For example, two dimensional (2D) nanomaterials like graphene and hexagonal boron nitride (h-BN)-based coatings have been reported as promising against prevention of corrosion [4–6]. These 2D materials are mechanically strong [7], flexible [8], good thermal conductors [9], have excellent chemical stability [10] and their coatings are impermeable [11] to gases and ions.

Surface modification and coatings of materials employed in biomedical applications help to improve biocompatibility, biocorrosion resistance and maximize functionality [12]. Deposition of thin films of titanium oxynitride and titanium oxynitride/Cu on wool by sputtering

was reported to regulate hydrophobicity, thermal stability and anti-bacterial activities of wool [13]. In the titanium nitride coatings produced by sputter coatings, the critical role of N/Ti ratio controls the films phase structure, growth orientation, morphology, contact angle, corrosion and biocompatibility [14]. Incorporation of third element in TiN coatings such as C, Si, Y, etc. can improve various properties of films. Ti–B–N coating consisting of 0.2 at.% of B displayed the highest hardness and the lowest wear rate [15]. Diamond like carbon (DLC) thin films deposited on steel substrates by pulsed direct current plasma enhanced chemical vapour deposition (pulsed-DC PE-CVD) can enhance the performance of stainless steel for biomedical applications [16]. In particularly, biocorrosion resistance of DLC films can be tailored by controlling the working parameter (bias voltage and deposition pressure) of PE-CVD process [12].

In the context of above discussion, boron nitride is also one of the nitride ceramic materials which could be attractive for surface modification and coatings of materials. Boron nitride (BN) is an inorganic ceramic material with wide band gap and astonishing properties [17]. BN compound is synthetically produced in ratio of 1:1 of B and N [18].

BN exists in both crystalline and amorphous forms, while BN have several crystalline varieties: cubic BN (c-BN), wurtzite BN (w-BN), hexagonal BN (h-BN) [18–20]. Hexagonal BN like graphene can exists in quasi-two-dimensional allotrope [21].

Boron nitride nanosheets (BNNS), a nanoform of h-BN, resembles graphene but it could be a better alternative to graphene as corrosion protection coating for metals because graphene coating have the ability to form galvanic cells with the metal due to its high electrical conductivity. In contrast, BNNS coatings due to their high electrical insulation nature can provide effective corrosion protection without the risk of galvanic cell formation with underlying metal [22]. Furthermore, BNNS is chemically inert, thermally stable and oxidation resistance, which are desired attributes for protection of metals against corrosion and environmental attack.

Several coating methods have been reported to develop BN coatings or its derivative such as BNNS, which include spin coating [22], dip coating [23], electrophoretic deposition (EPD) [24] and chemical vapour deposition (CVD) [25]. Husain et al. [22] developed spin coated BNNS on AISI 316 L SS for 24 h at 60 °C. The electrochemical studies indicated excellent corrosion inhibiting behavior of BN films. Sun et al. [23] dip-coated copper BNNS/poly vinyl butylene (PVB) paint and dried at 20 °C for 24 h before testing. Coating thickness was 27.7 ± 1.4 μm. They reported corrosion protection of BNNS/PVB coating increased with increase of BNNS loading in PVB. Song et al. [25] used copper (Cu) foil as a substrate and ammonia borane (AB) for producing h-BN nanosheets at 1000 °C for 40 min. They reported the resulting 2D films had a large optical band gap of 5.56 eV and showed high optical transparency in the UV–visible range. They believed that these films can be used as a dielectric to complement graphene devices. Ren et al. [26] deposited BNNS films on Cu using CVD. Monolayer and multilayers of BNNS were deposited by varying deposition time. Electrochemical tests verified good corrosion resistance of BNNS coatings in 3.5% NaCl solution. The research showed that BN films with adequate layers are good candidates for oxidation and corrosion protection. Kim et al. [27] demonstrated growth of highly crystalline, single-layer h-BN on platinum foil through a low-pressure CVD method using AB at 1100 °C that allowed h-BN to be grown over wide area (8×25 mm^2). The resulting BNNS′ thickness was 0.45 nm as determined by AFM and an optical band gap of 6.06 eV. The h-BN film also exhibited excellent insulating properties suggesting that it can be used as a dielectric layer. Liu et al. [28] developed large area and highly crystalline h-BN atomic layers (2–5 nm) via CVD method on nickel foil substrate (12.5 μm thick) at 1100 °C for 50 min in Ar/H$_2$ and AB atmosphere. They claimed that such ultrathin h-BN films would be impervious to oxygen diffusion even at high temperatures and can serve as high performance oxidation-resistant coatings for nickel up to 1100 °C in an oxidizing atmosphere. Chatterjee et al. [29] produced BNNS coatings on nickel (Ni) and Cu. Pakdel et al. [30] grown BNNS on silicon (Si)/silicon dioxide (SiO$_2$) by the passing NH$_3$ in CVD at 900–1200 °C for 60 min by using boron (B), magnesium oxide (MgO) and ferrous oxide (FeO) as precursor. Due to chemical inertness and the stability of the BNNS in a broad range of temperatures, they anticipated future industrial applications for the BNNS coating as super hydrophobic self-cleaning coatings. From the above discussion it can be noticed that CVD method has more potential for scalability and producing an effective BNNS coating on different substrates.

Previous studies focused on deposition of BNNS coatings on either Cu or Ni metals using precursors such as ammonia borane. The present study aims to deposit BNNS coating on mild steel using novel technique which involves reaction of boron powder and ammonia in CVD setup. The corrosion behavior of the BNNS coatings deposited on steel was studied with the aim to explore potential of these coatings for anti-corrosion applications. The reaction temperature and time were optimized to deposit BNNS coating on MS samples. BNNS coated-samples were characterized by X-ray diffraction (XRD), Fourier transform infrared spectroscopy (FTIR), scanning electron microscopy (SEM) and atomic force microscopy (AFM). The corrosion protection ability of BNNS coating was studied by Tafel analysis and electrochemical impedance spectroscopy (EIS) in 3.5% NaCl solution.

2. Experimental

2 1. Materials

Mild steel was used as a substrate for deposition of BNNS coating. Boron powder was purchased from US Research Nanomaterials, Inc. having particle size 1–2 μm and a purity of 99%. Ammonia gas was obtained from local industry.

2.2. Development of coating

Mild Steel (MS) samples were cut into 1×2 cm^2 strips and etched in 5% HCl solution. After etching, samples were sonicated and cleaned with 1 M NaOH solution. Boron powder (100 mg) was poured in a cleaned alumina boat, which was inserted in quartz tube of CVD furnace. The schematic of the apparatus used for coating is shown in Fig. 1(a). The MS sample to be coated was placed on the boat as shown in Fig. 1(b). After placing the boron-filled alumina boat and MS sample in the CVD furnace, quartz tube was closed from both ends and the tube was evacuated for 30 min. After reducing the pressure of the quartz tube down to 1 bar (0.1 MPa), ammonia gas was allowed to flow (200–250 sccm) through the quartz tube and temperature of the CVD furnace was increased from room temperature to 1200 °C at the rate of 50 °C per min (decided after series of experiments). After heating for the required time (30–180 min) at 1200 °C, CVD furnace was turned off and the coated samples were allowed to cool down to room temperature in the closed quartz tube for overnight. A photograph of the representative coated sample is shown in Fig. 1(b).

2.3. Characterization

The BNNS-coated MS samples were characterized for the coating morphology, composition roughness, and corrosion protection ability. BNNS coating structure was confirmed by XRD analysis. XRD patterns were obtained using diffractometer (Equinox 2000, Thermo Scientific) equipped with Ge monochromator and curved position sensitive detector. A coated sample was fixed on a bulk sample holder, which was placed on a spinning stage. Diffraction patterns were obtained using CuKα$_1$ radiation (0.1546 nm) in the region of 2θ° from 5° to 116° in real time for a total acquisition time of 10 min. FTIR was carried out using ATR mode by placing coated sample on diamond crystal (Shimadzu). Scanning electron microscopy (SEM, [Nova NanoSEM 450, FEG-SEM, FEI, Thermo Scientific, USA] was conducted to study coating morphology. Samples were sputter coated with gold prior to SEM analysis. Energy dispersive x-ray analysis (EDX) was carried out by EDAX system consisting of solid state detector having detection window of 25 mm^2. Semi-contact AFM (Nano-Solver, NT-MDT, Russia) was conducted to determine roughness and morphology of BNNS coating.

To study corrosion protection ability of BNNS coating, electrochemical testing was performed in three electrode system using potentiostat/galvanostat/ZRA (Reference 3000, Gamry Instruments, USA) in which BNNS coated-MS sample acted as working electrode, platinum wire as counter electrode and saturated calomel electrode (SCE) as reference electrode. All tests were performed in 3.5% NaCl solution. The samples to be tested had exposed area of 1 cm^2, area other than to be tested was insulated by polyester resin and electrical contact was made by soldering a Cu wire with the samples. For synchronized and comparable results, all samples were stabilized in the test solution (3.5% NaCl) after stabilization of open circuit potential (OCP), which took ca. 45 min and variation in OCP recorded was only ± 3 mV.

Tafel analysis was performed by applying over potential in anodic and cathodic directions in the range (-0.15 V–0.15 V (vs. OCP)) at scan rate of 1 mV/s. Electrochemical impedance spectroscopy (EIS) was
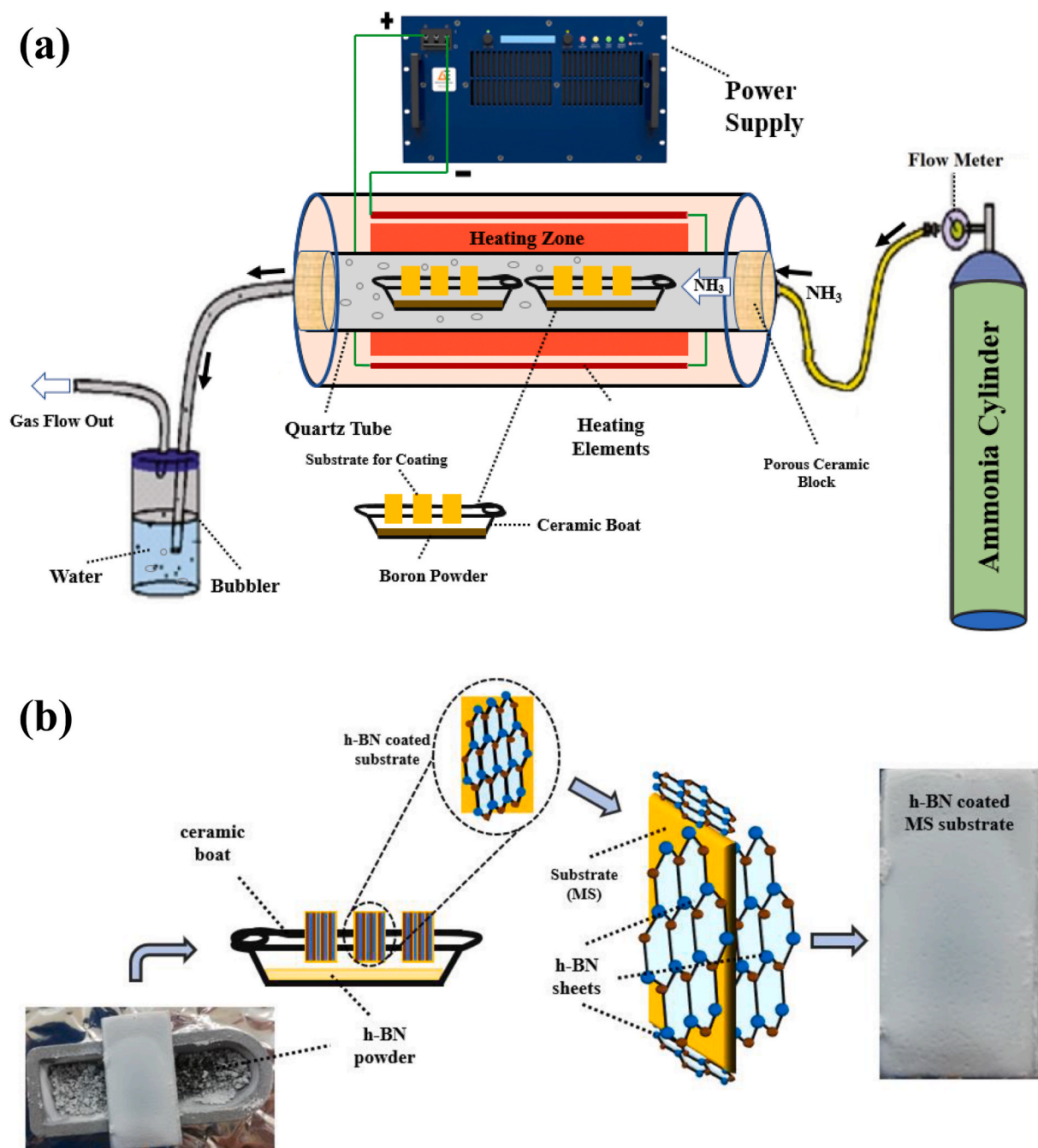
Fig. 1. Schematic of **(a)** CVD apparatus for coating of BNNS **(b)** BNNS coating on MS substrate.

performed in the frequency range 10 mHz–100 kHz with AC amplitude of ±10 mV (rms). Calculations for all electrochemical tests were done with the software (Echem, Analyst version 6.25, Gamry Instruments, USA).

3. Results and discussion

3.1. XRD

XRD patterns of bare MS and BNNS coated- MS samples are presented in Fig. 2. The effect of reaction time at fixed temperature of 1200 °C and placement of substrate sample in CVD furnace on the structure of BNNS coating is presented in Fig. 2. It can be seen from Fig. 2(b) that (002) peak of BN appeared in all the coated samples. The MS sample showed no peak in the $2\theta° = 26–27°$, which suggests BN was

coated on MS substrate [31]. It should also be noted that the MS sample placed in the reaction zone for 30 min had two peaks in the range of $2\theta°$ $= 26–27°$, while a single peak appeared from the coated samples kept in CVD furnace for reaction time of 1 and 3 h. The MS samples packed in the boron powder or placed above the powder made no difference, and in both cases (002) peak observed suggesting successful BN deposition on MS substrate. The (002) peak matched to that of h-BN in COD data base (COD Entry # 96-101-0603). XRD pattern of the boron powder recovered from alumina is presented in Fig. 3, which shows almost complete conversion of boron into BN. There was only a small peak of unreacted boron powder observed in the XRD pattern (Fig. 3) at about $2\theta = 39°$. We performed XRD analysis of the resulting powder (recovered from alumina boat) as shown in Fig. 3 and found that the BN powder had an average thickness of 6 nm as determined by Scherrer equation. The effect of microstrain was eliminated in the powder as well as coated
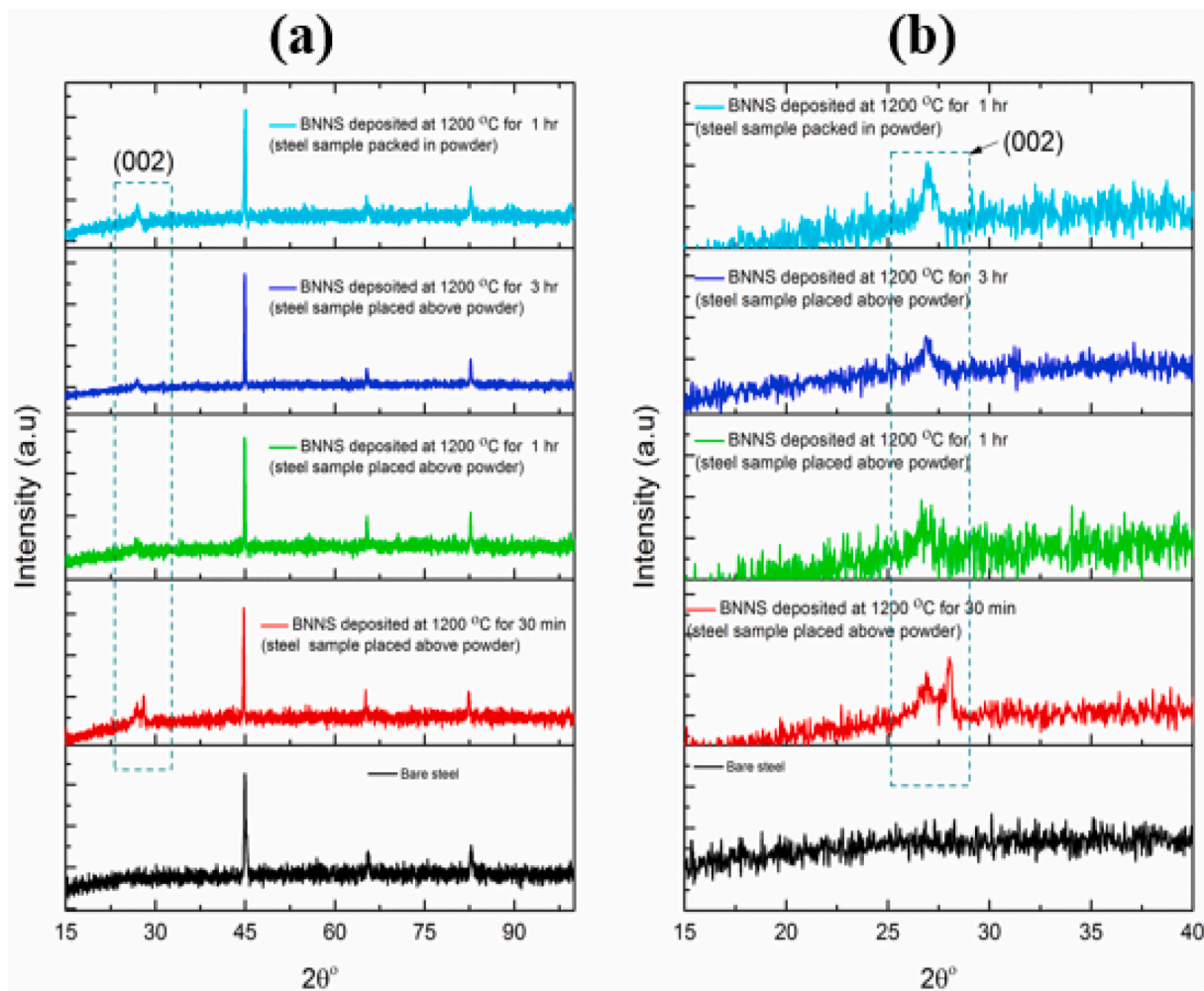
Fig. 2. XRD pattern of **(a)** BNNS coated-MS produced at 1200 °C for different reaction times and bare MS **(b)** zoomed section of (a) in the range $2\theta° = 26–27°$.
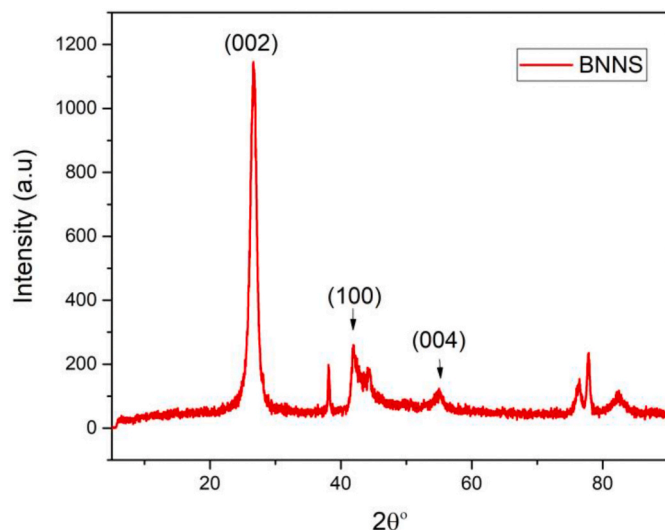

Fig. 3. XRD pattern of the powder obtained from alumina boat (BNNS).

samples due to their annealing in the furnace for overnight. This suggests BNNS formed by the reaction of boron and ammonia. Since the powder formed had BNNS like morphology, we called the resulting coating as BNNS coating.

3.2. FTIR and Raman spectroscopy

FTIR spectra of BNNS coated-MS samples produced at 1200 °C for different deposition times are presented in Fig. 4(a). A spectrum of commercial nanosized BN powder is also presented in Fig. 4(a) for comparison. In Fig. 4(a), there are two strong characteristic transmission peaks appeared at 1330 cm^{-1} and 760 cm^{-1} corresponding to sp^2-bonded B–N and B–N–B bending vibrations [32], respectively. The BNNS coated-MS samples at all temperatures showed these characteristic peaks of BN, confirming that BNNS deposition occurred at all temperatures irrespective of sample placement in the CVD furnace.

Raman spectra of BN (commercial) and BNNS coated-MS (1 h deposition time at 1200 °C) presented in Fig. 4(b) showed two characteristics peaks at 1377.69 cm^{-1} (BN) and 1366.49 cm^{-1} (BNNS coated-MS) which are related to the E$_{2g}$ vibration mode of BN [33]. A small shift of B–N bond peak in BNNS coated-MS than commercial BN (1366–1377 cm^{-1}) may be due to BN deposited as turbostratic nanosheets [34].

3.3. SEM and EDX

SEM images of bare MS and BNNS coated-MS produced at 1200 °C for 1 h reaction time (MS placed above boron powder) are shown in Fig. 5(a, c-d). SEM images of BNNS coated-MS samples clearly show deposition of BNNS on the surface of MS. Fig. 5(a) revealed that BNNS coating consisted of mainly BNNS (more than 80%), but some ribbons and boron nitride nanotubes (BNNTs) were also formed during deposition process. This could be possible because Fe of the substrate can play
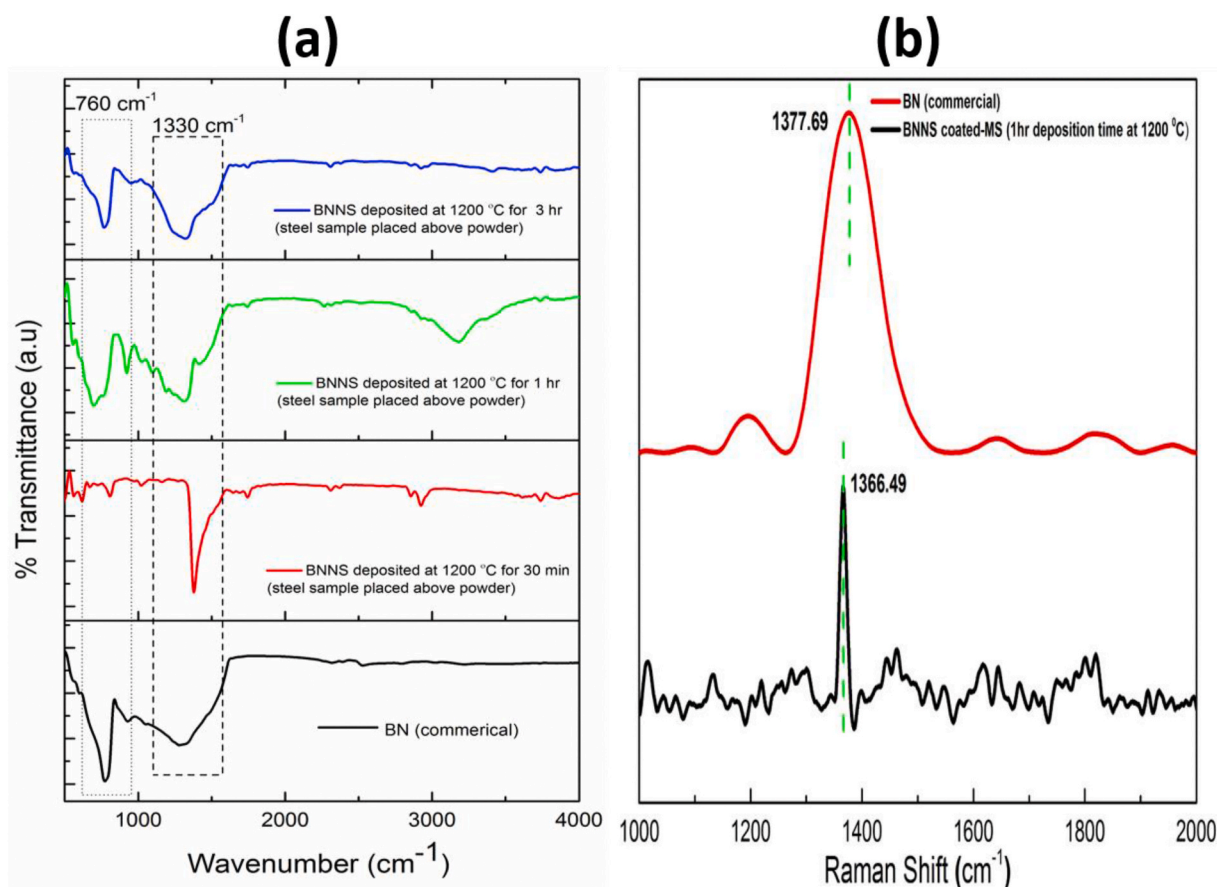
Fig. 4. (a) FTIR spectra of BN coated-MS produced at 1200 °C for different reaction times. FTIR spectrum of commercial BN (nanosized powder) is also presented for comparison and **(b)** Raman spectra of BN (commercial) and BNNS coated-MS (1 h deposition time at 1200 °C).

a role of catalyst for the growth of BNNTs [17]. Some pores in the coated sample are also noticeable as can be seen in Fig. 5(a). The high magnification images of coated MS (Fig. 5 (c & d)) revealed stacked sheet like morphology of the coating. An average thickness of BNNS coating deposited after 1 h of reaction time was found to be 28 µm as shown in Fig. 5(b).

EDX analyses of bare MS and BNNS coated-MS (1200 °C for 1 h) are shown in Fig. 6. As can be seen from Fig. 6(b), B and N were detected on the surface of BNNS coated-MS sample, which shows that BNNS was deposited on the MS substrate. It can also be noted that some oxygen was also detected in the coated sample, which depicts that some boron oxide may have also formed during the reaction. Although, we removed oxygen from CVD tube by vacuum pump, but the pressure was not reduced to great extent. It is believed that by reducing the oxygen pressure further in quartz tube, coating with high purity and improved morphology could be produced.

3.4. AFM

Semi-contact mode AFM images of bare MS and BNNS coated-MS sample produced at 1200 °C for 1 h reaction time are presented in Fig. 7. The AFM images of bare MS (Fig. 7 (a & b) show a rough surface before deposition. After deposition of coating, the surface of steel showed a different topography with much smoother and planar surface. Layers of BNNS can be seen in these images in the form of stacks, which are oriented in different directions suggesting trubostratic nature of the deposited BNNS. The random deposition of BNNS layers seems to develop some crevices or gaps between the layers which may be similar to pores observed in Figs. 5 and 6. The thickness of BNNS was found to be 5–6 nm which is in agreement with that obtained from XRD size

analysis [34].

3.5. Electrochemical characterization

3.5.1. Tafel analysis

Tafel curve of bare MS and BNNS coated-MS samples produced at 1200 °C for 1 and 3 h are shown in Fig. 8. Corrosion potential (E_{corr}) of BNNS coated-MS shifted towards more negative value, while corrosion current (I_{corr}) shifted to lower current than the bare MS. The decrease in corrosion current suggests that the BNNS hinders iron oxidation and enhances oxygen reduction [35]. Carbon and oxygen impurities are often present in BN crystals [36,37] and carbon doping from MS at high temperature (1200 °C) can form boron carbonitride which has found to be efficient in oxygen reduction [38,39]. The shift of corrosion potential to more negative side were also previously reported by Husain et al. [22] and Li et al. [5]. The negative potential shift implies that BNNS coating acted as cathodic coating to MS and did not favour galvanic corrosion due to their electrical insulation, which is highly likely in the case of graphene coating [5]. Kinetic parameters obtained from Tafel curves' analysis are shown in Table 1. It can be seen from Table 1 that E_{corr} increased for both samples coated for 1 and 3 h, whereas the I_{corr} decreased compared to bare MS. The I_{corr} for a BNNS coated-MS sample produced at 1200 °C for 1 h decreased from 32.00 µA/cm^2 to 15.9 µA/cm^2, which shows 2 times improvement in corrosion resistance of BNNS coated-MS. The corrosion rate of the sample coated for 1 h was found lower than the one coated for 3 h.

3.5.2. EIS

EIS was performed to understand electrochemical behavior of BNNS coated-MS and to validate Tafel analysis results. Nyquist and Bode plots
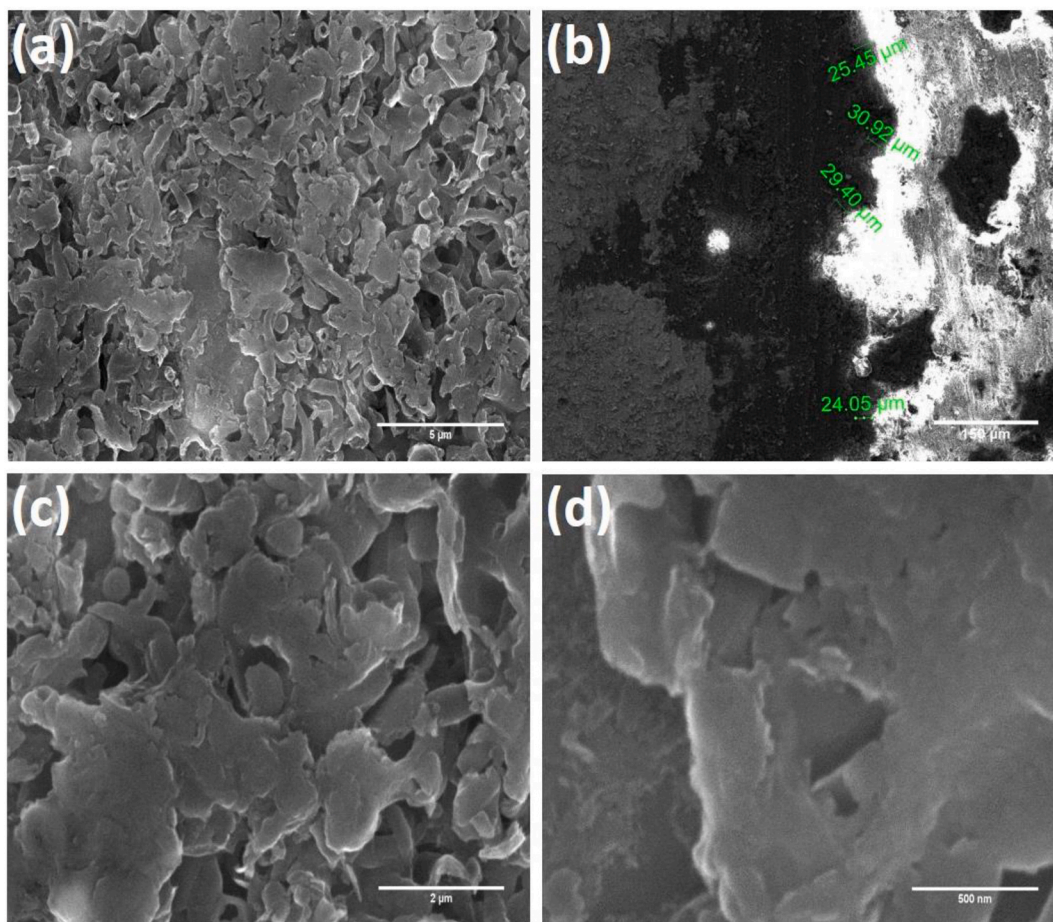
Fig. 5. SEM images **(a–d)** BNNS coated-MS and **(b)** thickness of BNNS coating deposited on MS sample produced at 1200 °C for 1 h reaction time.
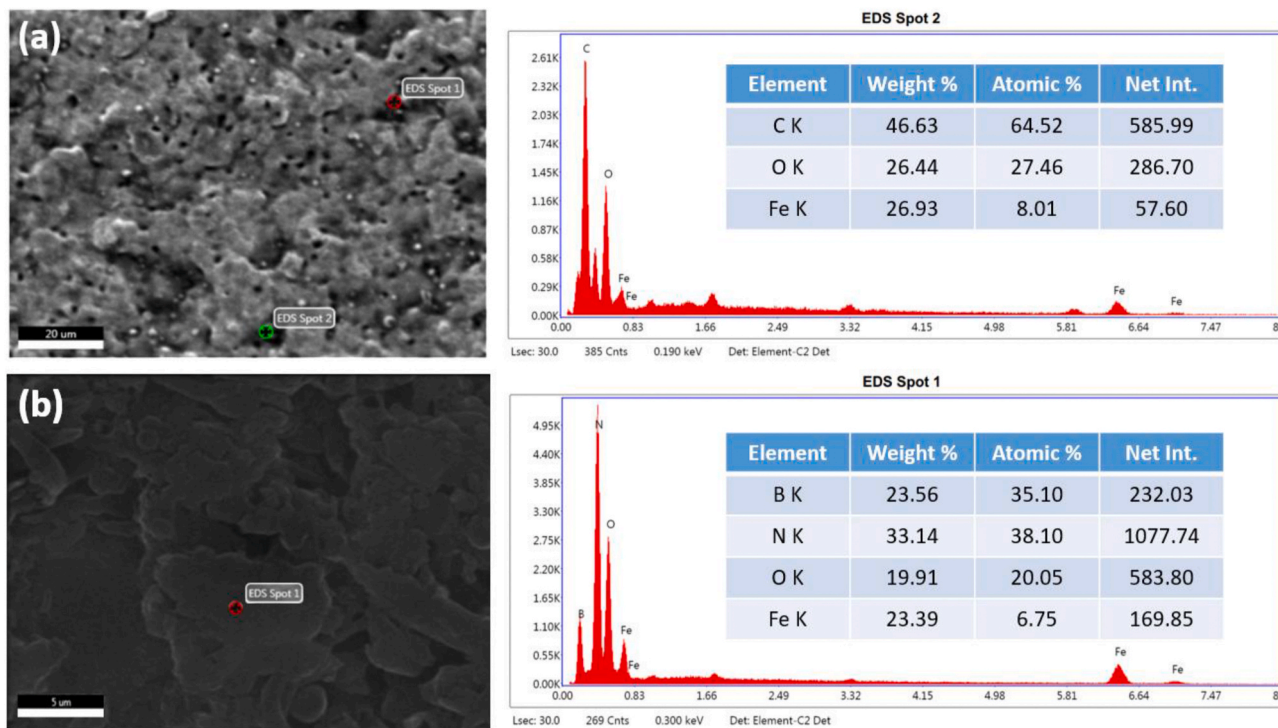

Fig. 6. EDS analysis **(a)** Bare MS sample **(b)** BNNS coated-MS sample produced at 1200 °C for 1 h reaction time.
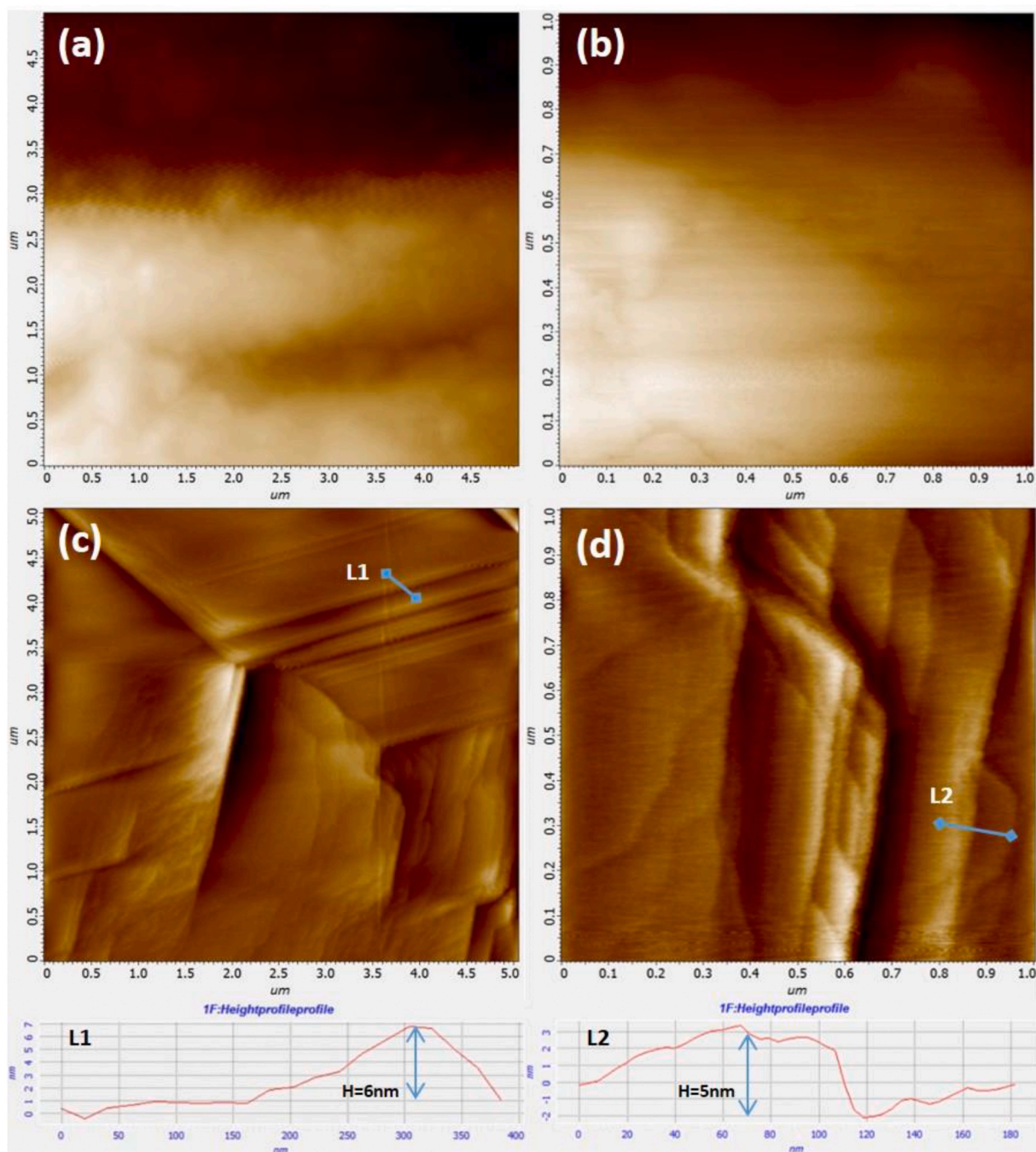
Fig. 7. AFM images of **(a, b)** bare MS sample and **(c, d)** BNNS coated-MS samples with height profile produced at 1200 °C for 1 h reaction.

of bare MS and BNNS coated-MS at 1200 °C for 1 h are shown in Fig. 10. A larger semi-circle in Nyquist plot of BN coated-MS shows its higher impedance than bare MS, suggesting good corrosion protection and low ion penetration ability of BNNS coating. For quantitative estimation of anticorrosion performance of BNNS coated-MS, electrical equivalent circuit models shown in Fig. 9 were fitted to EIS curves (by using Echem analyst 7.03 software) shown in Fig. 10 [24]. In the circuit shown in Fig. 9, R_{sol}, R_c, R_{ct}, C_c and C_{dl} represents solution resistance, coating resistance, charge-transfer resistance, coating capacitance and double-layer capacitance, respectively. Their values obtained after fitting of model are listed in Table 2. In the case of bare MS, corrosive medium has to attack MS through the double layer which forms around the metal when corrosive medium interacts with the surface, while in the case of BNNS coated- MS sample the corrosive medium faces

tortuous path to reach at the surface of substrate due to barrier provided by stacked BNNS. Here, corrosive medium faces two major resistances to complete its path to the metal: First is the coating resistance and the second is R_{ct} (between coating and metal surface) [40] as illustrated in Fig. 9.

It can be seen from Table 2 that the value of R_{ct} for bare MS and BNNS coated-MS are 298.8 Ωcm^2 and 1996.3 Ωcm^2, respectively. The increase of R_{ct} indicates improvement in the corrosion protection ability of BNNS coating by ca. 6.6 × compared to bare MS. This result is in agreement with Tafel results. The higher value of C_{dl} for BNNS coated-MS than bare MS implies that the exposure of the MS surface in the case of BNNS coating to corrosive medium (O_2, H_2O, Cl^-) is limited than the bare MS [24].

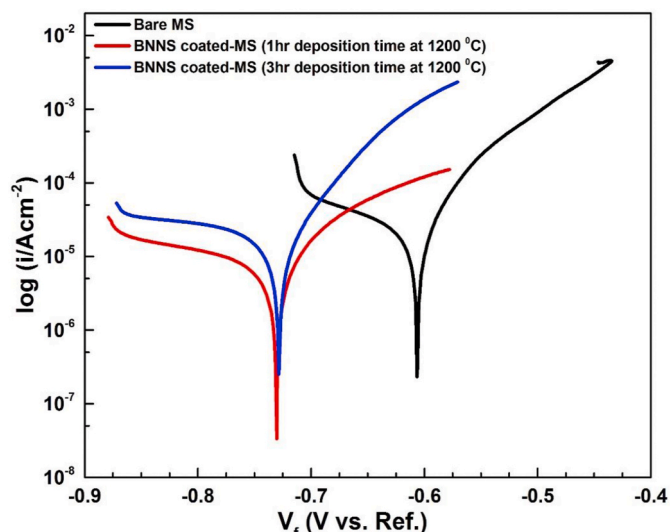Generally, the impedance modulus at lowest frequency is an

Fig. 8. Tafel curves of bare MS and BNNS coated-MS samples (produced at 1200 °C for 1 and 3 h) in 3.5% NaCl solution.

Table 1
Kinetic parameters calculated from Tafel analysis.

Sample name	E_{corr} (mV)	I_{corr} (μA/cm^2)	Corrosion Rate (mpy)
Bare MS	−606.0	32.00	14.75
BNNS coated MS (1 h deposition time)	−731.0	15.90	7.337
BNNS coated-MS (3 h deposition time)	−728.0	24.60	11.37

important parameter to evaluate the corrosion resistance of coating, and higher impedance value suggests higher resistance to corrosion. From bode plot in Fig. 10, it can been seen that BNNS coated-MS showed higher initial impedance modulus (2.43×10^3 Ωcm^2), while the bare MS shows lower initial impedance modulus ($Z_f = 0.01$ Hz), 323.5 Ωcm^2,

suggesting an outstanding physical barrier offered by BNNS coating to corrosive medium (O_2, H_2O, Cl^-) which would result in longer-term corrosion protection of MS [40].

4. Conclusions

An inorganic ceramic BN-based coating was successfully deposited on MS samples by reaction of boron powder and ammonia gas in CVD furnace. A uniform white colored coating was deposited on the samples at temperature of 1200 °C for the reaction time of 1 h. Both FTIR and Raman spectroscopy of the coating confirmed deposition of BN on MS samples. XRD analysis confirmed that deposited coating was primarily consisted of hexagonal boron nitride, and the BN powder formed along with the coating was found to have a thickness of 6 nm as determined by Scherrer equation. SEM revealed that the as-deposited coating mainly comprised of BN nanosheets, but some nanoribbons or nanotubes were also found in the coating. AFM analysis of the coated samples confirmed sheet like morphology of the deposited coating with the thickness of about 5–6 nm in agreement with XRD analysis. The BNNS coating was tested for its anticorrosion performance in 3.5% NaCl solution using Tafel analysis and EIS. On the basis of Tafel analysis, it was found that corrosion rate of bare mild steel decreased from 14.75 to 7.33 mpy, corresponding to 2 × improved corrosion resistance ability of BNNS coated-MS. EIS analysis showed that BNNS coating had higher impedance and 6 × more charge transfer resistance than bare MS implying superior corrosion protection ability offered by BNNS coating. The BNNS coating due to its two dimensional morphology and stacking parallel to the substrate formed a tortuous path for the ingress of the electrolyte to the substrate helping in enhancing corrosion resistance of MS. The study highlights that BNNS coating can be a promising ceramic coating for protecting steel against aggressive aqueous corrosion.

Credit author statement

Aamir Nadeem: Investigation, Formal analysis, Writing - original draft. Muhammad Faheem Maqsood: Investigation, Formal analysis, Writing - original draft. Mohsin Ali Raza: Conceptualization, Supervision, Funding acquisition, Writing - review & editing. Muhammad Tasaduq Ilyas: Experimental setup design, Formal analysis Javaid Iqbal:
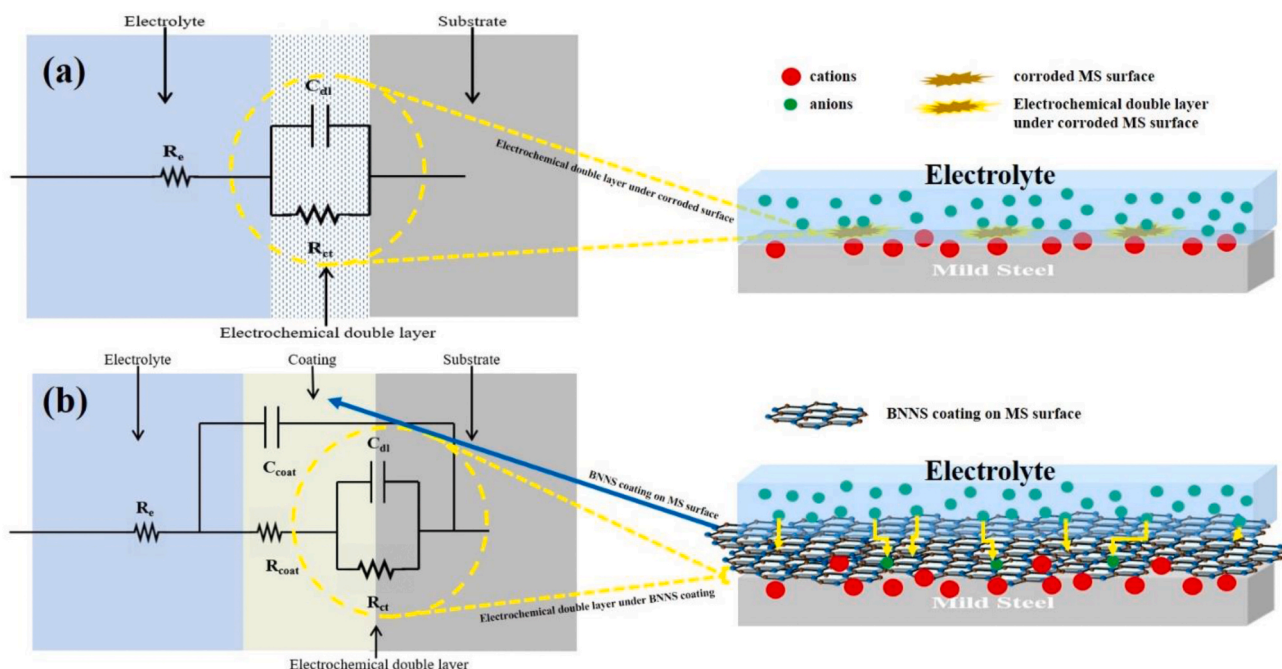
Fig. 9. Schematic of electrical equivalent circuits of **(a)** bare and **(b)** BNNS coated MS sample and corresponding illustration of corrosion process.
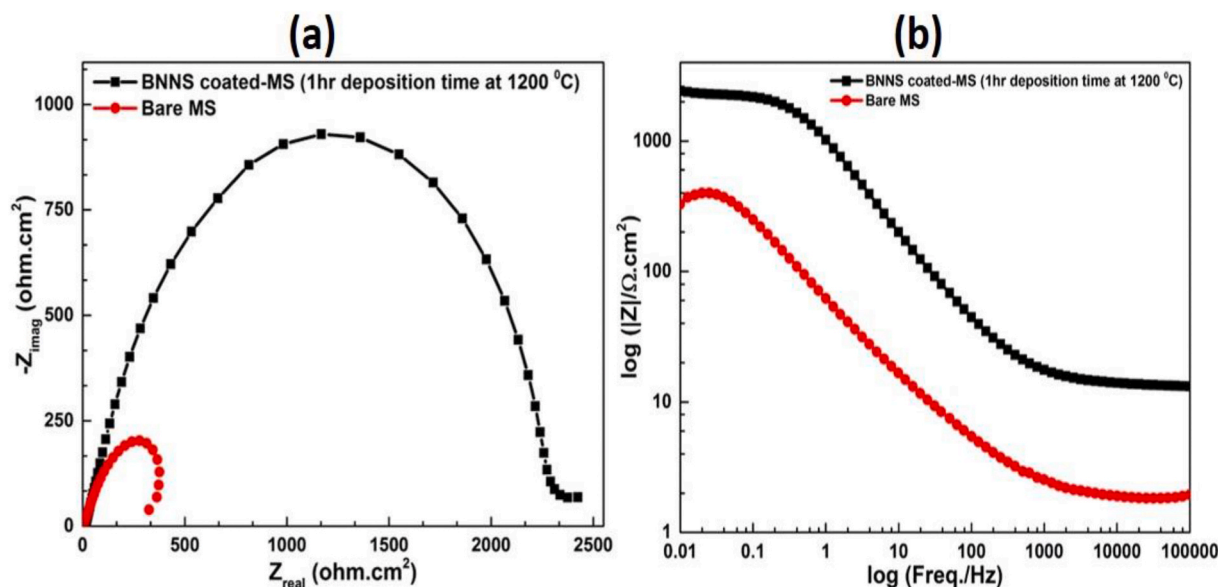
Fig. 10. (a) Nyquist plots, **(b)** Bode plots of bare MS and BNNS coated-MS deposited at 1200 °C for 1 h.

Table 2
Kinetic parameters calculated after fitting of EIS data to electrical equivalent circuits.

Sample name	R_{sol} (Ωcm^2)	R_c (Ωcm^2)	R_{ct} (Ωcm^2)	C_c (Fcm^2)	C_{dl} (Fcm^2)	Goodness of fit
Bare MS	2.18	–	298.8	–	2.538e-3	2.17e-3
BNNS coated-MS (1 h deposition time)	2.55	137.1	1996.3	35.84e-6	87.96e-6	1.71e-3

Formal analysis, review & editing, Visualization. Zaeem Ur Rehman: Investigation, Software.

Declaration of competing interest

Acknowledgement

References

[1] Koch, G.H., et al., *Corrosion Cost and Preventive Strategies in the United States.* 2002, United States. Federal Highway Administration.
[2] M. Segarra, et al., Copper and CuNi alloys substrates for HTS coated conductor applications protected from oxidation. Materials Science Forum, Trans Tech Publications Ltd., Zurich-Uetikon, Switzerland, 2003.
[3] M. Redondo, C.B. Breslin, Polypyrrole electrodeposited on copper from an aqueous phosphate solution: corrosion protection properties, Corrosion Sci. 49 (4) (2007) 1765–1776.
[4] S. Böhm, Graphene against corrosion, Nat. Nanotechnol. 9 (10) (2014) 741.
[5] L.H. Li, et al., Boron nitride nanosheets for metal protection, Advanced materials interfaces 1 (8) (2014) 1300132.
[6] M.A. Raza, et al., Corrosion study of electrophoretically deposited graphene oxide coatings on copper metal, Thin Solid Films 620 (2016) 150–159.
[7] C. Zhi, et al., Large-scale fabrication of boron nitride nanosheets and their utilization in polymeric composites with improved thermal and mechanical properties, Adv. Mater. 21 (28) (2009) 2889–2893.
[8] S.J. Kim, et al., Materials for flexible, stretchable electronics: graphene and 2D materials, Annu. Rev. Mater. Res. 45 (2015) 63–84.
[9] A.A. Balandin, et al., Superior thermal conductivity of single-layer graphene, Nano Lett. 8 (3) (2008) 902–907.
[10] K.D. Sattler, Handbook of Nanophysics: Functional Nanomaterials, CRC Press, 2010.
[11] K.S. Novoselov, et al., A roadmap for graphene, nature 490 (7419) (2012) 192.

[12] M.R. Derakhshandeh, et al., Diamond-like carbon-deposited films: a new class of biocorrosion protective coatings, Surface Innovations 6 (4–5) (2018) 266–276.
[13] M. Sadeghi-Kiakhani, et al., Thermally stable antibacterial wool fabrics surface-decorated by TiON and TiON/Cu thin films, Surface Innovations 6 (4–5) (2018) 258–265.
[14] A. Nemati, et al., Magnetron-sputtered TixNy thin films applied on titanium-based alloys for biomedical applications: composition-microstructure-property relationships, Surf. Coating. Technol. 349 (2018) 251–259.
[15] I. Asempah, et al., Microstructure, mechanical and tribological properties of magnetron sputtered Ti-BN films, Surf. Eng. 35 (8) (2019) 701–709.
[16] M.R. Derakhshandeh, et al., Diamond-like carbon thin films prepared by pulsed-DC PE-CVD for biomedical applications, Surface Innovations 6 (3) (2018) 167–175.
[17] A. Pakdel, et al., Low-dimensional boron nitride nanomaterials, Mater. Today 15 (6) (2012) 256–265.
[18] X.-F. Jiang, et al., Recent progress on fabrications and applications of boron nitride nanomaterials: a review, J. Mater. Sci. Technol. 31 (6) (2015) 589–598.
[19] S. Bernard, P. Miele, Nanostructured and architectured boron nitride from boron, nitrogen and hydrogen-containing molecular and polymeric precursors, Mater. Today 17 (9) (2014) 443–450.
[20] M. Kawaguchi, S. Kuroda, Y. Muramatsu, Electronic structure and intercalation chemistry of graphite-like layered material with a composition of BC6N, J. Phys. Chem. Solid. 69 (5–6) (2008) 1171–1178.
[21] J.C. Meyer, et al., Selective sputtering and atomic resolution imaging of atomically thin boron nitride membranes, Nano Lett. 9 (7) (2009) 2683–2689.
[22] E. Husain, et al., Marine corrosion protective coatings of hexagonal boron nitride thin films on stainless steel, ACS Appl. Mater. Interfaces 5 (10) (2013) 4129–4135.
[23] W. Sun, et al., Communication—multi-layer boron nitride nanosheets as corrosion-protective coating fillers, J. Electrochem. Soc. 163 (2) (2016) C16–C18.
[24] H.-R. Zhao, J.-H. Ding, H.-B. Yu, Phosphorylated boron nitride nanosheets as highly effective barrier property enhancers, Ind. Eng. Chem. Res. 57 (42) (2018) 14096–14105.
[25] L. Song, et al., Large scale growth and characterization of atomic hexagonal boron nitride layers, Nano Lett. 10 (8) (2010) 3209–3215.
[26] S. Ren, et al., Multilayer regulation of atomic boron nitride films to improve oxidation and corrosion resistance of Cu, ACS Appl. Mater. Interfaces 9 (32) (2017) 27152–27165.
[27] G. Kim, et al., Growth of high-crystalline, single-layer hexagonal boron nitride on recyclable platinum foil, Nano Lett. 13 (4) (2013) 1834–1839.
[28] Z. Liu, et al., Ultrathin high-temperature oxidation-resistant coatings of hexagonal boron nitride, Nat. Commun. 4 (2013) 2541.
[29] S. Chatterjee, et al., Chemical vapor deposition of boron nitride nanosheets on metallic substrates via decaborane/ammonia reactions, Chem. Mater. 23 (20) (2011) 4414–4416.
[30] A. Pakdel, et al., Boron nitride nanosheet coatings with controllable water repellency, ACS Nano 5 (8) (2011) 6507–6515.

[31] L.H. Li, et al., Large-scale mechanical peeling of boron nitride nanosheets by low-energy ball milling, J. Mater. Chem. 21 (32) (2011) 11862–11866.

[32] Z. Cui, et al., Large scale thermal exfoliation and functionalization of boron nitride, Small 10 (12) (2014) 2352–2355.

[33] O.Y. Posudievsky, et al., Efficient dispersant-free liquid exfoliation down to the graphene-like state of solvent-free mechanochemically delaminated bulk hexagonal boron nitride, RSC Adv. 6 (52) (2016) 47112–47119.

[34] X. Li, et al., Exfoliation of hexagonal boron nitride by molten hydroxides, Adv. Mater. 25 (15) (2013) 2200–2204.

[35] E. Sherif, S.-M. Park, Inhibition of copper corrosion in 3.0% NaCl solution by N-phenyl-1, 4-phenylenediamine, J. Electrochem. Soc. 152 (10) (2005) B428–B433.

[36] L. Li, et al., High-quality boron nitride nanoribbons: unzipping during nanotube synthesis, Angew. Chem. Int. Ed. 52 (15) (2013) 4212–4216.

[37] Y. Kubota, et al., Deep ultraviolet light-emitting hexagonal boron nitride synthesized at atmospheric pressure, Science 317 (5840) (2007) 932–934.

[38] S. Wang, et al., BCN graphene as efficient metal-free electrocatalyst for the oxygen reduction reaction, Angew. Chem. Int. Ed. 51 (17) (2012) 4209–4212.

[39] Y. Zheng, et al., Two-step boron and nitrogen doping in graphene for enhanced synergistic catalysis, Angew. Chem. Int. Ed. 52 (11) (2013) 3110–3116.

[40] Y. Wu, et al., Synergistic functionalization of h-BN by mechanical exfoliation and PEI chemical modification for enhancing the corrosion resistance of waterborne epoxy coating, Prog. Org. Coating 142 (2020) 105541.